

Hubbard U library and high throughput exploration of spin Hamiltonian parameters for the rational design of metal trihalides MX_3 ($\text{M}=\{\text{Ti},\text{V},\text{Cr},\text{Fe}\}$, $\text{X}=\{\text{Cl},\text{Br},\text{I}\}$) with high Curie temperature.

Dorye L. Esteras, José J. Baldoví *

Instituto de Ciencia Molecular (ICMol), Universidad de Valencia,
Catedrático José Beltrán 2, 46980 Paterna, Spain.

ABSTRACT: Metal trihalides (MX_3) are the most important family of 2D magnetic materials, being the chromium trihalides the most studied 2D magnets. The discovery of CrI_3 , the recent obtention of CrCl_3 in-plane magnetic monolayer and the role of CrBr_3 inducing topological superconductivity in NbSe_2 , may serve to showcase the active research being done in this family nowadays. Despite the high impact of these materials, most of the members in the MX_3 family are still unexplored and constitute an untapped source of interesting physical properties. Stimulated by the most recent advances in straintronics and aware of the crucial role of the dielectric screening, we present here a high throughput methodology to automatize the exploration of 2D materials. Employing this methodology, we studied the MX_3 family ($\text{M}=\text{Cr}, \text{Fe}, \text{V}, \text{Ti}$; $\text{X}=\text{Cl}, \text{Br}, \text{I}$) with the goal of advancing towards the solution of the most problematic issue in these materials, namely the Curie temperature. We use a particular case to show how this methodology allows us to obtain a complete description of the magnetic interaction picture ($J_{\text{iso}}, J_{xx}, J_{yy}, J_{zz}$) up to third neighbors condensed in a single effective equation per parameter, describing magnetic interaction in terms of the strain and the Hubbard U parameter. Additionally, and because of the important role of the Hubbard U in MX_3 materials, we provide a library of self-consistent calculated Hubbard U for the principal pseudopotential families. The work presented herein advances in the description of the still unexplored MX_3 materials, opening the door to a rational design of 2D magnetic materials.

2D magnetic materials provide an excellent platform to realize the hottest topics in condensed matter science, such as spintronics and quantum computation^[1,2] They also provide a plethora of interesting phenomena such as topological properties and Moiré magnets^[3,4]. Also nascent fields as magnonics and straintronics find in 2D magnetic materials, a perfect environment to explore new properties of matter^[5-8]. Looking more in depth in the field of 2D materials, metal trihalides (MX_3) are the most important family, being chromium trihalides the most studied 2D magnets^[8-11]. The discovery of CrI_3 ^[13], the recent obtention of CrCl_3 in-plane magnetic monolayer^[14] and the role of CrBr_3 inducing topological superconductivity in NbSe_2 ^[14], may serve to showcase the active research being done in this family nowadays. Despite the high impact of these materials, most of the members in the MX_3 family are still unexplored and constitute an untapped source of interesting physical properties.

In opposition to the numerous advantages of these materials, the temperature necessary to maintain the magnetic order (Curie temperature) has shown to be specially low, being the most problematic issue of the family. Different approaches have been studied to improve this limitation^[15-17]. Among the strategies to obtain materials with improved properties, recent studies have shown the key role of strain and dielectric screening manipulation. Biaxial strain has raised as an important method to improve the properties of 2D materials^[18, 19]. On the other hand, to tune the properties of different systems modifying the dielectric screening using the Hubbard U parameter could provide important results as shown in recent works^[20]. An important ad-

vantage of these techniques is to provide an easy implementation using different substrates to apply certain dielectric screening and biaxial strain conditions.

To obtain a detailed exploration of MX_3 materials under the effect of these techniques using ab initio calculations is still limited by four important problems. First, the Hubbard model has a crucial role in the description of these systems, and is often not well considered. The absence of self-consistent Hubbard U parameters has produced in the community a tendency to use U values not properly calculated, which belong to calculations with a different pseudopotential, structure or even a different material. On the other hand, the obtention of the magnetic interaction parameters is not trivial, these parameters are often calculated using the total energy map analysis which requires the use of big supercells to take account of high order interaction. This ends in a high cost description in terms of simple Hamiltonians. Another important problem is related to Curie temperature, which calculation is often performed using classical methods as Monte Carlo simulations, or even with very simple analytical laws. Despite all these methods are able to provide correct results in most of the cases, a different approach is needed to perform a high throughput study of these properties, looking for a less expensive, easier to automatize and more precise method.

Herein, we perform a high throughput exploration of the MX_3 family ($\text{M}=\text{Cr}, \text{Fe}, \text{V}, \text{Ti}$; $\text{X}=\text{Cl}, \text{Br}, \text{I}$) to propose a different strategy to address these issues. We provide a self-consistent Hubbard U library for different pseudopotentials in the case of each material in order to encourage the use of a correct Hubbard

U. We use Wannier90^[21] to connect our QuantumEspresso^[22] DFT+U calculations with the Green function method, recently implemented in TB2J software^[23], to obtain an inexpensive mapping into a Heisenberg Hamiltonian. With the magnetic interaction data acquired, we use a recently developed code^[24] to obtain T_c as a solution of the quantum Heisenberg model in applied field conditions taking account up to third neighbors. Finally, to show that the accuracy and reliable cost of this method offers a solution to the high computational cost required to perform a full study of these materials, we perform a deeper study in the case of CrCl_3 under strain and Hubbard U modifications. This methodology allows us to obtain a very complete description of the CrCl_3 magnetic scenario and allows us to map the magnetic exchange and anisotropies up to third neighbors into effective equations providing an easy and instantaneous way to obtain an accurate approximation of the magnetic parameters under -5% to 5% strain conditions and in a 2-6 eV Hubbard U range. With this complete description of the system we are able to provide an infinite resolution heat map for Curie temperature, probing this approach as a valuable method for the rational design of 2D materials.

RESULTS AND DISCUSSION

The Hubbard model is a key element to describe the Mott-Hubbard physics present in magnetic systems and thus a correct estimate of the Hubbard U becomes crucial. Despite of this, a complete self-consistent calculation of the Hubbard U parameters has not yet been performed for MX_3 materials. As a consequence, the Hubbard U is usually extracted from a given calculation and then transferred to a calculation that relies on different codes or pseudopotentials or even is applied to different materials. To address this problem, we performed DFT calculations over the MX_3 monolayer slab structures in order to calculate and converge the self-consistent Hubbard U for some of the most used families of pseudopotentials (see details in the Methods section). The Projected Augmented Wave (PAW) and “ultrasoft” (US) families of pseudopotentials from the QuantumEspresso^[22] database are specially interesting because they provide a relativistic version of the pseudopotential, something needed to properly perform spin-orbit calculations using a Hubbard U that is consistent with the selected pseudopotential. Additionally, the Materials Cloud^[25] database pseudopotentials were analyzed (in this particular case, GBRV^[26] and PAW pseudopotentials were recommended) to calculate the Hubbard U. The results of this study are presented in Table 1, which could be used as a self-consistent calculated Hubbard U library. We take advantage of these results to point out the strongly dependence of the Hubbard U with the pseudopotential. We can see the differences are not always critical if we compare PAW and US pseudopotentials but the difference could be very severe if we compare the Hubbard U obtained with other pseudopotentials as the ones provided by the GBRV^[26] library (shown in this paper), or with norm-conserving pseudopotentials. Due to the importance of spin orbit coupling in this work, from this point onwards we employ exclusively PAW and US pseudopotentials.

Although the Hubbard U depends mostly on the metallic core, it is also affected by the exchange-correlation functional and the chemical environment of the localized orbitals. In our results we observe a tendency in the self-consistent U depending on the halide (figure 1). This tendency is independent from the

pseudopotentials chosen and characteristic for each metal ion, increasing with rising atomic radius of the halide in the case of Cr^{3+} and Fe^{3+} halides, with halides of Ti^{3+} and V^{3+} presenting the opposite behavior. In all cases, the U ranges between 3.7 - 4.9 eV depending on the material. The evolution of the Hubbard U with respect to the pseudo-potential, metal ion and halide is well behaved, so that if any particular calculation does not converge it can be estimated with reasonable accuracy by knowing the results of neighbouring calculations. This fact allows to predict the Hubbard U for the different structures as we did in the case of non-converging calculations (TiI_3 , TiBr_3 , VI_3) with the US pseudopotentials. Thus, we think the Hubbard U library provided could be used to predict also the non-calculated values, if an interpolation of the Hubbard U values between the different pseudopotentials, metallic cores and halides is performed.

Table 1. Self-consistent Hubbard U library for MX_3 . PAW and US pseudopotentials provided by the QuantumEspresso database and the US pseudopotentials provided by the GBRV library.

MX_3	PP type	PP name	U (eV)
TiCl₃	PAW	Ti.pbe-spn-kjpaw_psl.1.0.0.UPF	4.150
	US	Ti.pbe-spn-rrkjus_psl.1.0.0.UPF	4.142
TiBr₃	PAW	Ti.pbe-spn-kjpaw_psl.1.0.0.UPF	3.992
	GBRV	ti_pbe_v1.4.uspp.F.UPF	5.444
TiI₃	PAW	Ti.pbe-spn-kjpaw_psl.1.0.0.UPF	3.775
VCl₃	PAW	V.pbe-spn1-kjpaw_psl.1.0.0.UPF	4.817
	US	V.pbe-spn1-rrkjus_psl.1.0.0.UPF	4.819
	GBRV	v_pbe_v1.4.uspp.F.UPF	4.803
VBr₃	PAW	V.pbe-spn1-kjpaw_psl.1.0.0.UPF	4.698
	US	V.pbe-spn1-rrkjus_psl.1.0.0.UPF	4.714
	GBRV	v_pbe_v1.4.uspp.F.UPF	4.682
VI₃	PAW	V.pbe-spn1-kjpaw_psl.1.0.0.UPF	4.615
	GBRV	v_pbe_v1.4.uspp.F.UPF	4.592
CrCl₃	PAW	Cr.pbe-spn-kjpaw_psl.1.0.0.UPF	3.775
	US	Cr.pbe-spn-rrkjus_psl.1.0.0.UPF	3.802
	GBRV	cr_pbe_v1.5.uspp.F.UPF	4.990
CrBr₃	PAW	Cr.pbe-spn-kjpaw_psl.1.0.0.UPF	3.887
	US	Cr.pbe-spn-rrkjus_psl.1.0.0.UPF	3.912
	GBRV	cr_pbe_v1.5.uspp.F.UPF	5.170
CrI₃	PAW	Cr.pbe-spn-kjpaw_psl.1.0.0.UPF	3.992
	US	Cr.pbe-spn-rrkjus_psl.1.0.0.UPF	4.015
	GBRV	cr_pbe_v1.5.uspp.F.UPF	5.393
FeCl₃	PAW	Fe.pbe-spn-kjpaw_psl.1.0.0.UPF	4.056
	US	Fe.pbe-spn-rrkjus_psl.0.2.1.UPF	3.952
FeBr₃	PAW	Fe.pbe-spn-kjpaw_psl.1.0.0.UPF	4.161
	US	Fe.pbe-spn-rrkjus_psl.0.2.1.UPF	4.062
FeI₃	PAW	Fe.pbe-spn-kjpaw_psl.1.0.0.UPF	4.209
	US	Fe.pbe-spn-rrkjus_psl.0.2.1.UPF	4.119

In the following calculations we will use the US pseudopotentials and a structurally self-consistent U, as proposed by Hsu et al^[27] while enforcing the MX_3 monolayer structures to be optimized with the calculated U. Following this DFT+U approach, we performed self-consistent calculations adding spin-orbit coupling (see details in the Methods section). As can be seen in the calculated electronic band structures (Figure 2), MX_3 is a family of Mott insulators^[28, 29] meaning the band gap strongly depends on the Hubbard U. In this extreme case of the

Mott-Hubbard physics an incorrect use of the Hubbard U predicts a metal as previously reported in most of these materials. Considering the well-known difficulties of DFT+ U to predict the gap the procedure leads overall to satisfactory results. We need to note that according to our calculations TiX_3 and VX_3 behave as semiconductors, but due to the limitations of DFT to correctly predict the Mott insulator behavior we cannot be certain whether the metallic prediction for the other VX_3 is accurate or masked by an insufficiently accurate calculation of the Fermi level. Furthermore, our calculation underestimates the band gap in the case of CrI_3 , whereas by cancellation of errors one would obtain the right answer for the band gap (1.2 eV) if one did not perform the optimization process using the Hubbard U . Finally, for simplicity, to facilitate comparisons and since it is the most common behavior, in our calculations we assume ferromagnetic coupling in all cases. Note that theoretical studies have predicted AFM behavior in the case of FeX_3 ^[30] this can constitute a limitation of the present study.

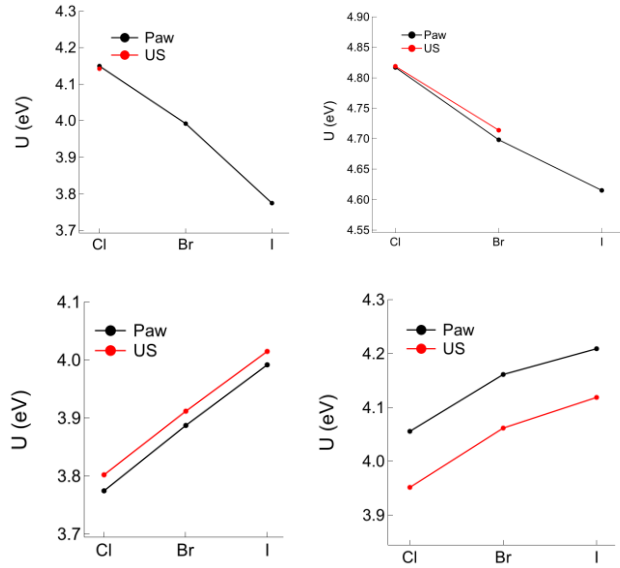


FIGURE 1. Self-consistent Hubbard U as a function of the halide. On the top of the figure a decreasing tendency is observed in Ti^{3+} (left) and V^{3+} (right). The opposite tendency is observed on the bottom of the figure in the case of Cr^{3+} (left) and Fe^{3+} (right).

In addition to the DFT+ U calculations, Wannier90^[21] software allows to project the physics of the Bloch orbital-based picture in terms of maximally localized orbitals represented by the Wannier functions. The DFT+ U +SOC calculations are then mapped into a tight binding Hamiltonian expressed in the maximally localized Wannier function basis (equation 1), where we chose as projectors the d orbitals of the metals and the p orbitals of the halides (see details in the Methods section). Equation 1 represents the definition of Wannier function where the U operator rotates the wavefunction basis to look for the maximally localized wavefunction basis set. Finally this set is expressed in a real space description by the inverse Fourier transform.

$$|\mathbf{R}n\rangle = \frac{V}{(2\pi)^3} \int_{\text{BZ}} d\mathbf{k} e^{-i\mathbf{k}\cdot\mathbf{R}} \sum_{m=1}^J U_{mn}^{(\mathbf{k})} |\psi_{m\mathbf{k}}\rangle \quad (1)$$

where \mathbf{R} denotes the Wannier function, n the energy index and \mathbf{k} the wave vector. As shown by different authors, the magnetic interactions in the few explored cases of the metal trihalide family show a complex microscopic origin^[31]. Here we use our DFT+ U calculations expressed in the Wannier90 tight binding Hamiltonian to reduce the full many body electronic interaction problem into an effective Heisenberg Hamiltonian (Equation 2). In order to achieve this, recently TB2J software^[23] has provided the community with a different procedure, which employs Green functions to avoid the previously used total energy mapping analysis. This method not only provides another important connexion with Wannier90, but also, as we show in this work, opens the door to a low cost and easy to automatize procedure to calculate the magnetic interaction in materials science. Equation 2 contains four energy terms. The first one corresponds to the single ion anisotropy which is followed by the isotropic and anisotropic exchange terms. The last term corresponds to the Dzyaloshinskii–Moriya interaction. In this equation \mathbf{S}_i denotes the spin vectors normalized to 1.

$$E = - \sum K_i (\vec{S}_i \cdot \vec{e}_i)^2 - \sum [J_{ij}^{iso} \vec{S}_i \cdot \vec{S}_j + \vec{S}_i J_{ij}^{ani} \vec{S}_j + \vec{D}_{ij} \cdot (\vec{S}_i \times \vec{S}_j)] \quad (2)$$

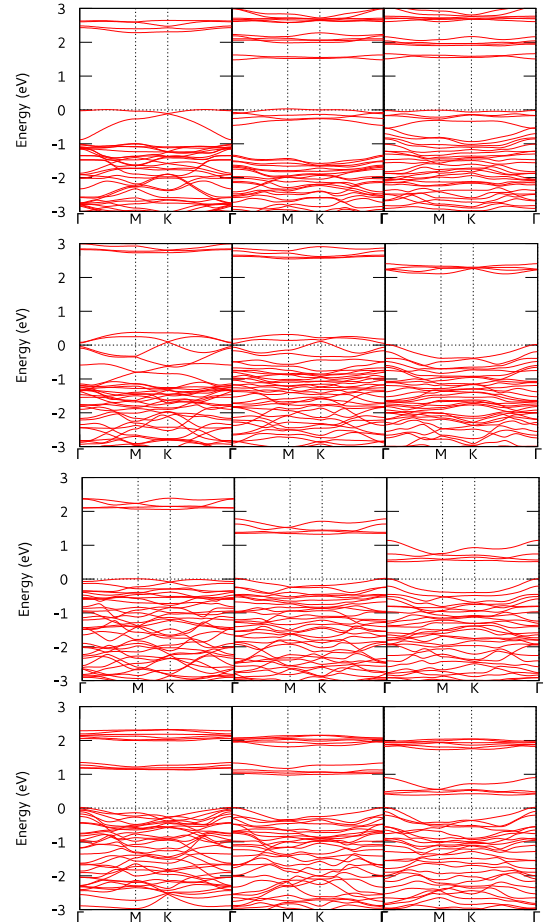


FIGURE 2. DFT+ U +SOC electronic band structure of MX_3 , left to right Cl, Br and I structures are shown and from the top to the bottom Ti^{3+} , V^{3+} , Cr^{3+} , Fe^{3+} .

TBJ provides an easy connection to calculate the Curie temperature via Montecarlo simulations using the software Vampire^[32] However, to benchmark our calculations, we assume a quantum mechanical approach as proposed by Vanherck^[24], using our previous calculations to solve a quantum Heisenberg model (Equation 3, 4) considering the anisotropic exchange interaction up to the third neighbors and the effect of a magnetic field applied in arbitrary direction as represented in equation 3. Equation 3 decomposes the system in a Zeeman Hamiltonian and a quantum Heisenberg spin Hamiltonian detailed in equation 4. In equation 4 the spin Hamiltonian is described in terms of a global exchange J and the anisotropy Δ , considering the system as an effective lattice of spins where d index runs up to third neighbors. The results obtained from the combination of these two codes is present in the supporting information where table 2 shows the magnetic parameters and the calculated T_c for each MX_3 system.

$$\hat{H} = \hat{H}_B + \hat{H}_{\text{ex}} \quad (3)$$

$$\hat{H}_{\text{ex}} = -\frac{1}{2} \sum \sum J_{1d} [(1 - \Delta_{1d})(\hat{S}_d^x \hat{S}_1^x + \hat{S}_d^y \hat{S}_1^y) + (1 + \Delta_{1d})\hat{S}_d^z \hat{S}_1^z] \quad (4)$$

where S_d^j represents the j spin component of the d neighbor. As mentioned above, one of the advantages of this methodology is its suitability to perform a high throughput study connecting techniques that are inexpensive and easy to automatize. To showcase this, we focused in a detailed analysis of CrCl_3 to provide a complete description of the magnetic picture and map the path to enhancing the Curie temperature. A recent experiment has shown the monolayer limit can be achieved with CrCl_3 keeping his magnetic properties^[13] which are specially interesting due to the in-plane ferromagnetic order. In addition, recent experiments have observed spin waves in this material^[33]. The possibility to manipulate the magnetic exchange and anisotropies with different techniques as strain or modification of the dielectric screening make CrCl_3 an interesting candidate for magnonics. Herein we explore the effects of applying a comprehensive and extensive biaxial strain up to a 5% in either direction (compression/expansion) and of the modification of the dielectric screening via varying the Hubbard U parameter in a 2-6 eV range. Strains in this range are expected to be below the breaking conditions of these materials, given the good mechanical properties in the monolayer regime. In contrast, the explored window in the case of the Hubbard U is very wide, and should serve to provide an exploration of the limits in these materials; probably realistic values of U will be in a much narrower range.

We analyzed all magnetic parameters obtained in this study of CrCl_3 (J_{iso} , J_{xx} , J_{yy} , J_{zz}). These results show a near-linear response of the interaction parameters to a change of the strain and/or the Hubbard U , and indeed, they provide sufficient information to calculate the Curie temperature in very different scenarios. But also, they provide enough information to understand the non-trivial dependence of the magnetic parameters in terms of the strain and Hubbard U at the same time. Simple polynomials were able to describe the behaviour of the magnetic parameters respect to the Hubbard U , with the evolution of the coefficients in this polynomials were described with functions in terms of the strain, as shown in equation 5.

Equation 5 presents, the general form of each of the 12 magnetic parameters under study (F), and $k_i(s)$ the function which describes the coefficients of F in terms of the strain. The description of the third order parameters was noisy but due to the low values of these parameters were able to reproduce them without a significant error. We think in the extreme case of high U and high extensive strain the model finds its limits, so a non-highly accurate prediction is expected in this scenario. This approach allows to condensate the whole magnetic interaction picture in the form of effective equations. These effective equations successfully reproduce the behavior of the anisotropic exchange up to third neighbors and provide an instantaneous technique to obtain the magnetic parameters in a wide range of dielectric screening and strain conditions of this material. With this complete description of the magnetic picture of CrCl_3 , we are able to obtain infinite values of T_c , in figure 3 we provide a heat map of Curie temperature for 2040 values of strain and the Hubbard U provided by the effective equations in the range of calculated values (95%-105% lattice constants and 2-6 eV Hubbard U). This fully resolved Curie map presented in figure 3 describes the evolution of the Curie temperature in different conditions, some of which might be accessible via a correct substrate selection.

$$F = k_0(s) + k_1(s)U + k_2(s)U^2 \quad (5)$$

$$k_i(s) = c_0 + c_1s + c_2s^2 + c_3s^3$$

where k_i are coefficients of order i for the polynomial expansion of F as a function of U and c_i are coefficients for the polynomial expansion of k_i as a function of strain s . A more detailed explanation and the full list of coefficients are presented in the supporting information.

If we observe figure 3, we can see how the Curie temperature increases with strain and the dielectric screening. The effect of strain could increase the Curie temperature by up to 40%, as was suggested by previous reports^[34]. One needs to point out that even if a high strain is applied, that could result in a zero T_c increase if the dielectric screening is not correctly tuned. This means the real effect of strain as a powerful tool to improve the properties of materials could be impeded in several scenarios, by the screening effect of a certain substrate. Another remarkable detail is that in the limit of low Hubbard U and high compression, we obtain that CrCl_3 becomes an in plane ferromagnet then a negative out of plane spontaneous magnetization produces a vanishing T_c in the model used. This is a very interesting result if we think that the in-plane behavior of CrCl_3 is not properly described with DFT as shown in various works^[35]. We think DFT is not able to successfully reproduce this behavior in CrCl_3 , but also that the effect of strain and screening contributes to the in-plane spin configuration of this material in the experiments.

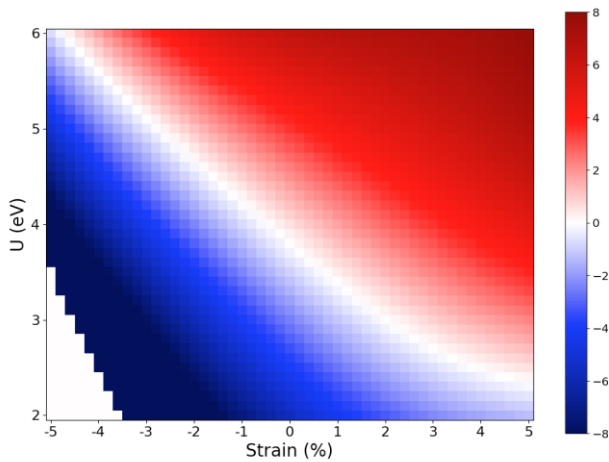


FIGURE 3. High resolved ΔT_c map (2040 values of strain and Hubbard U). In the range of low Hubbard U and low strain CrCl_3 is predicted as an in-plane ferromagnet (white zone at the bottom), then T_c is not properly calculated. The reference for ΔT_c is $T_c = 23.19$ K calculated at $U = 3.8$ eV, 0% strain.

CONCLUSIONS

We presented herein a high throughput exploration of metal trihalides MX_3 for $M = \{\text{Ti}, \text{V}, \text{Cr}, \text{Fe}\}$, $X = \{\text{Cl}, \text{Br}, \text{I}\}$. We provided a library of self-consistent Hubbard U for PAW, US and GBRW for this set of metal trihalides. For all of these systems, we calculated the main parameters of the Heisenberg spin Hamiltonian, namely isotropic exchange and exchange anisotropy components xx , yy and zz , for first, second and third nearest neighbours and from these we calculated the Curie temperature. Crucially, we systematically repeated these calculations multiple times in the case of CrCl_3 , covering a bidimensional parameter space where one dimension is the Hubbard U and the second is a biaxial strain of the lattice constants. This results in an effective equation description of the abovementioned parameters of the Heisenberg spin Hamiltonian. This allows to easily predict the magnetic parameters in a wide range of dielectric screening and applied strain. From these calculations we were able to establish, for each of the parameters in the effective Hamiltonian, an effective equation as a function of U and the strain, allowing predictive heat maps. The methodology presented herein provides an accurate but inexpensive technique to explore new materials. A simple script was able to perform all the DFT calculations and combine the results with the Hamiltonian study, showing that this method provides an efficient strategy to perform high throughput studies in the field of 2D materials.

Methods

First-principle calculations were performed based on density functional theory (DFT) as implemented in the Quantum Espresso code^[22]. The generalized gradient approximation (GGA) and the Perdew–Burke–Ernzerhof functional^[36] were used to describe the exchange–correlation energy. To properly describe the Mott–Hubbard physics present in these systems we adopted a DFT + U approach where U is the on-site Coulomb repulsion, using the simplified version proposed by Dudarev et al^[37]. The

self-consistent calculation of the Hubbard U was performed following the method proposed by Cococcioni et al^[38, 39]. until the Hubbard U parameter was converged to 0.01 eV. These parameters were used to fully optimize the monolayer structures, previously isolated by 18 Å of vacuum. The optimization was realized using a ‘2Dxy’ restriction until the forces in each atom and the energies differences were converged attending to the materials cloud efficient criteria in each particular case. The optimized structures were used to simulate the effect of a biaxial strain through the modification of the in-plane lattice parameters, also the Hubbard U was modified in a 0 to 6 eV range. In each of these cases, self-consistent calculations using spin-orbit coupling were carried out converging the results to 10^{-6} Ryd. The Brillouin zone was sampled by a well converged Γ centered $9 \times 9 \times 1$ k-point Monkhorst–Pack mesh^[40] for all calculations. At this stage, Wannier90 software^[21] was used to describe the systems in terms of a tight-binding Hamiltonian were 56 Wannier functions were used to describe the 20 d orbitals of the metals and the 36 p orbitals of the halides. The calculations were well converged along a $9 \times 9 \times 1$ Wigner-Seitz supercell, using 50 Wannierisation steps to obtain highly atom centered Wannier functions and the spreads were always less than 1 Å in the d orbitals and less than 2 Å in the p orbitals.

In order to describe the magnetic interaction of these systems, the Green function method was used as implemented in TB2J software^[23]. The interaction was performed along a converged $9 \times 9 \times 1$ mesh, and the contour integral was solved using 500 steps and a correct value of ϵ_{max} depending on the metallic or insulator behavior of the system. The anisotropic exchanges between the metallic cores were obtained as a result of the average between DFT+U+Wannier90 calculations with the spins along the three special directions. Finally, to calculate the Curie temperature, the quantum Heisenberg model was solved as shown by Vanherck et al^[24].

To obtain a correct description of the magnetic parameters expressed in effective equations, we fit the different magnetic parameters using a maximum of order 2 polynomials to describe the dependence with the Hubbard U. The evolution of these polynomial coefficients needed up to 3 order expansion in some cases (see details in Supplementary Information). We systematically calculate more data until we were able to predict the new parameters obtained.

ACKNOWLEDGMENT

This work has been supported by the COST Action MolSpin on Molecular Spintronics (Project 15128), H2020 (FATMOLS project) and QUANTERA (SUMO project), the Spanish MINECO (grants MAT2017-89993-R and CTQ2017-89528-P cofinanced by FEDER and Excellence Unit María de Maeztu CEX2019-000919-M), and the Generalitat Valenciana (Prometeo Program of Excellence and CDEIGENT/2019/022). We thank A. Gaita-Ariño for the helpful discussion.

REFERENCES

- [1] E. C. Ahn, npj 2D Mat. Appl. 2020, 4, 17
- [2] E. Coronado, Nature Reviews Materials 2020, 5, 87–104
- [3] E. Y. Andrei, D. K. Efetov, P. Jarillo-Herrero, A. H. MacDonald, K. F. Mak, T. Senthil, E. Tutuc, A. Yazdani, A. F. Young, Nature Reviews Materials 2021, 6, 201–206
- [4] K. Hejazi, Z.-X. Luo, L. Balents, PNAS 2020, 117, 1072110726.
- [5] A. Barman, S. Mondal, S. Sahoo, A. De, J. Appl. Phys. 2020, 128, 170901
- [6] S. Chakraborty, A. Ravikumar, Sci. Rep. 2021, 11, 198

- [7] A. V. Sadovnikov, A. A. Grachev, S. E. Sheshukova, Yu. P. Sharaevskii, A. A. Serdobintsev, D. M. Mitin, S. A. Nikitov, *Phys. Rev. Lett.* 2018, 120, 257203
- [8] D. Ghazaryan, M.T. Greenaway, Z. Wang, V.H. Guarochico-Moreira, I.J. Vera-Marun, J. Yin, Y. Liao, S. V. Morozov, O. Kristanovski, A. I. Lichtenstein, M. I. Katsnelson, F. Withers, A. Mishchenko, L. Eaves, A. K. Geim, K. S. Novoselov, A. Misra. *Nature Electronics* 2018, 1, 344–349.
- [9] D. Soriano, M. I. Katsnelson, J. Fernández-Rossier, *Nano Lett.* 2020, 20, 6225–6234.
- [10] M.A. McGuire, *Crystals* 2017, 7, 121.
- [11] B. Huang, G. Clark, D. R. Klein, D. MacNeill, E. Navarro-Moratalla, K. L. Seyler, N. Wilson, M. A. McGuire, D. H. Cobden, D. Xiao, W. Yao, P. Jarillo-Herrero, X. Xu, *Nature Nanotechnology* 2018, 13, 544–548.
- [12] B. Huang, G. Clark, E. Navarro-Moratalla, D. R. Klein, R. Cheng, K. L. Seyler, D. Zhong, E. Schmidgall, M. A. McGuire, D. H. Cobden, W. Yao, D. Xiao, P. Jarillo-Herrero, X. Xu, *Nature* 2017, 546, 270–273.
- [13] A. Bedoya-Pinto, Jing-Rong Ji, A. Pandeya, P. Gargiani, M. Valvidares, P. Sessi, F. Radu, K. Chang, S. Parkin, arXiv:2006.07605 (2020).
- [14] S. Kezilebieke, Md N. Huda, V. Vaño, M. Aapro, S. C. Ganguli, O. J. Silveira, S. Głodzik, A. S. Foster, T. Ojanen, P. Liljeroth, *Nature* 2020, 588, 424–428.
- [15] Y. Ren, Q. Li, W. Wan, Y. Liu, Y. Ge, *Phys. Rev. B* 2020, 101, 134421
- [16] F. Subhan, J. Hong, *J. Phys. Chem. C* 2020, 124, 7156–7162
- [17] H. Li, Y.-K. Xu, K. Lai, W.-B. Zhang, *Phys. Chem. Chem. Phys.*, 2019, 21, 11949–11955
- [18] F. Carrascoso, R. Frisenda, A. Castellanos-Gomez *Nano Materials Science* (2021), <https://doi.org/10.1016/j.nanoms.2021.03.001>
- [19] A. Castellanos-Gomez, R. Roldán, E. C., M. Buscema, F. Guinea, H. S. J. van der Zant, and G. A. Steele, *Nano letters* 2013, 13, 5361–5366.
- [20] M. Rösner, J. L. Lado. *Phys. Rev. Research* 2021, 3, 013265.
- [21] A. A. Mostofi, J. R. Yates, Young-Su Lee, I. Souza, D. Vanderbilt, N. Marzari, *Comp. Phys. Commun.* 2008, 178, 685–699.
- [22] P. Giannozzi, S. Baroni, N. Bonini, M. Calandra, R. Car, C. Cavazzoni, D. Ceresoli, G. L. Chiarotti, M. Cococcioni, I. Dabo, *J. Phys. Cond. Matt.* 2009, 21, 395502.
- [23] X. He, N. Helbig, M. J. Verstraete, E. Bousquet, *Comp. Phys. Commun.* 2021, 264, 107938.
- [24] J. Vanherck, C. Bacaksiz, B. Sorée, M. V. Milošević, W. Magnus, *Appl. Phys. Lett.* 2020, 117, 052401.
- [25] L. Talirz, S. Kumbhar, E. Passaro, A. V. Yakutovich, V. Granata, F. Gargiulo, M. Borelli, M. Uhrin, S. P. Huber, S. Zoupanos, C. S. Adorf, C. W. Andersen, O. Schütt, C. A. Pignedoli, D. Passerone, J. VandeVondele, T. C. Schulthess, B. Smit, G. Pizzi, N. Marzari, *Scientific Data*, 2020, 7, 209
- [26] K.F. Garrity, J.W. Bennett, K.M. Rabe and D. Vanderbilt, *Comput. Mater. Sci.*, 2014, 81, 446
- [27] H. Hsu, K. Umemoto, M. Cococcioni, R. Wentzcovitch, 2009 *Phys. Rev. B* 79, 125124
- [28] J. Geng, I. N. Chan, H. Ai, K. H. Lo, Y. Kawazoe, K. W. Ng, H. Pan, *Physical Chemistry Chemical Physics*, 2020, 22 (17)
- [29] F. Subhan, J. Hong, *J. Phys.: Condens. Matter*, 2020, 32, 245803
- [30] S. Tomar, B. Ghosh, S. Mardanya, P. Rastogi, B.S. Bhadoria, Y. S. Chauhan, A. Agarwal, S. Bhowmick, *Journal of Magnetism and Magnetic Materials*, 2019, 489, 165384
- [31] J. L. Lado, J. Fernández-Rossier, *2D Materials*, 2017, 4.3, 035002
- [32] R. F. L. Evans, W. J. Fan, P. Chureemart, T. A. Ostler, M. O. A. Ellis and R. W. Chantrell, *J. Phys.: Condens. Matter*, 2014, 26, 103202
- [33] Kapoor, Lucky N., S. Mandal, P. C. Adak, M. Patankar, S. Manni, A. Thamizhavel, M. M. Deshmukh, *Advanced materials*, 2020, 33(2), 2005105.
- [34] L. Webster, J. Yan, *Phys Rev Lett B*, 2018, 98, 144411
- [35] F. Xue, Y. Hou, Z. Wang, R. Wu, *Phys Rev Lett B*, 2019, 100, 224429
- [36] J. P. Perdew, K. Burke, M. Ernzerhof *Phys. Rev. Lett.*, 1996, 77, 3865
- [37] S. L. Dudarev, G. A. Botton, S. Y. Savrasov, C. J. Humphreys, and A. P. Sutton, *Phys. Rev. B*, 1998, 57, 1505
- [38] M. Cococcioni, and S. De Gironcoli, *Physical Review B*, 2005, 71.3, 035105.
- [39] I. Timrov, N. Marzari, M. Cococcioni, *Physical Review B*, 2018, 98.8, 085127.
- [40] H. J. Monkhorst, J. D. Pack, *Phys. Rev. B*, 1976, 13, 5188

